Liquid Crystals
Publication details, including instructions for authors and subscription information:
http://www.informaworld.com/smpp/title~content=t713926090

Physical characterization of B1 and B2 phases in a newly synthesized series of banana shaped molecules

J. P. Bedel; J. C. Rouillon; J. P. Marcerou; M. Laguerre; M. F. Achard; H. T. Nguyen

Online publication date: 06 August 2010

To cite this Article Bedel, J. P. , Rouillon, J. C. , Marcerou, J. P. , Laguerre, M. , Achard, M. F. and Nguyen, H. T.(2000) 'Physical characterization of B1 and B2 phases in a newly synthesized series of banana shaped molecules', Liquid Crystals, 27: 1, 103 — 113
To link to this Article: DOI: 10.1080/026782900203272
URL: http://dx.doi.org/10.1080/026782900203272

LIQUID CRYSTALS, 2000, VOL. 27, NO. 1, 103–113

Physical characterization of B1 and B2 phases in a newly synthesized series of banana shaped molecules

J. P. BEDEL, J. C. ROUILLON, J. P. MARCEROU, M. LAGUERRE†,
M. F. ACHARD* and H. T. NGUYEN

Centre de Recherche Paul Pascal, Université Bordeaux I, Av. A. Schweitzer,
33600 Pessac, France
†Institut Européen de Chimie et Biologie,
Ecole Polytechnique-Université Bordeaux I-Université II, Avenue Pey-Berland,
33402 Talence, France

(*Received 17 June 1999; accepted 28 July 1999*)

A new homologous series of achiral banana-shaped mesogens ('C*n*') has been synthesized and studied by classical techniques (optical microscopy, differential scanning calorimetry, X-ray diffraction and electro-optic investigations). Complete miscibility with compounds of the *n*-OPIMB series shows that the short homologues (C5–C9) exhibit a frustrated B1 antiphase, while the longer members (C10–C14) present a B2 smectic C phase. Electro-optic measurements confirm this identification.

1. Introduction

Until recently, the observation of ferroelectricity in liquid crystals, resulting in macroscopic electric polarization, was restricted to materials with a chiral molecular structure. But in 1996, Niori *et al.* [1] reported that ferroelectricity was observed in a smectic phase formed by bent achiral molecules. Since then, 'banana-shaped' mesogens have turned into a major liquid crystal subfield and several groups are currently working on these materials [2–11]. Nevertheless, only minor modifications of the initial structure ('PIMB series' [3]), such as the insertion of a lateral group on the central ring [6, 8], have been reported up to now.

As part of our continuing effort to establish the molecular structure/mesomorphic property relationships for liquid crystalline materials, we have synthesized several series of banana shaped materials of general formula:

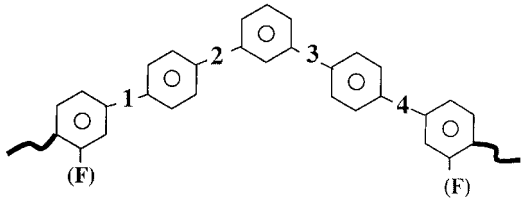

*Author for correspondence;
e-mail: achard@crpp.u-bordeaux.fr

where two mesogenic units are connected to the 1- and 3-positions of the central benzene ring. The linking groups labelled '1, 2, 3, 4' are either ester (−COO− or −OCO−) or thioester (−COS− or S−CO−) or imino (−CH=N− or −N=CH−) groups. Within this representation, molecules are symmetric when groups 1 and 4 are the same *and* 2 and 3 are the same. Materials are said to be non-symmetric when 1 differs from 4, or 2 differs from 3. The terminal tails are alkoxy or ester chains. Some series possess a fluorine on an external ring.

As a main result of these different syntheses, we have observed mesomorphic properties in series where the donor or acceptor nature of the four linking groups leads to an alternate sequence of positive and negative charges on the five phenyl rings. This molecular architectural model appears to give a necessary condition to induce mesomorphic order [12]. However many chemical modifications remain suitable and small changes can greatly modify the mesomorphic properties. Complex polymorphism can be observed and the phase identification remains in many cases uncertain. Thus, for the sake of simplicity, we choose to present in this paper a new series of banana-shaped molecules which exhibit only a liquid crystalline *mono*morphism.

Liquid Crystals ISSN 0267-8292 print/ISSN 1366-5855 online © 2000 Taylor & Francis Ltd
http://www.tandf.co.uk/journals/tf/02678292.html

2. Materials

The new symmetric banana-shaped molecules ('Series C') correspond to the general formula:

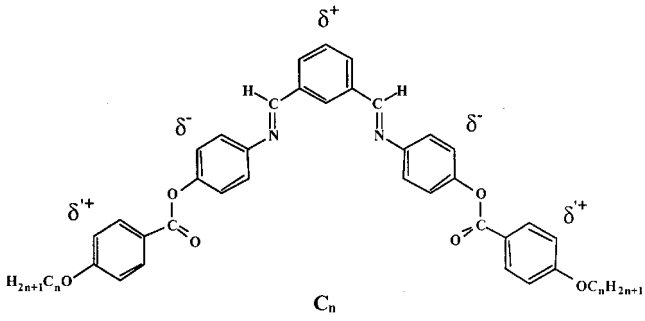

Cn

with $n = 5$–14. The materials are labelled 'C*n*', where *n* is the number of carbon atoms in the terminal alkoxy chain. They differ from the *n*-OPIMB reference series [2, 3] in the position and the directional sense of the linking groups. Indeed, in these molecules the azomethine groups are linked to the 1,3-positions of the central phenyl ring and the ester groups are placed between the outside phenyl rings. The alternating distribution of the charges on the five phenyl rings is respected, according to our molecular architectural model. As previously mentioned, this model appears to be a necessary condition to obtain liquid crystalline phases in banana-shaped molecules. In series C, the charge alternation is the same as in the series reported in [11] and is opposite to the alternation in the *n*-OPIMB series.

Note that the corresponding non-symmetric series 'series I' (with '1' = −COO−, '2' = −OCO−, '3' = −CH=N− and '4' = −OCO−) has been previously published and some results are given for comparison [11]. In the same manner, the materials are labelled 'I*n*' for symmetric chains.

The members of the 1,3-phenylene bis[4-(4-*n*-alkoxybenoyloxy)phenyliminomethyl] family (series C*n*) were synthesized according to the scheme in figure 1.

Isophthaldehyde (0.1 mol) and 4-aminophenol (0.2 mol) were dissolved in boiling absolute ethanol in the presence of a few drops of acetic acid. The solution was heated at reflux for 3 h. This condensation led to the 1,3 phenylene bis(4-hydroxyphenyliminomethyl) (**1**), which was recrystallized three times from a heptane/ethanol mixture. To obtain the members of series C*n*, the appropriate 4-*n*-alkoxybenzoic acid (2 mmol) and compound **1** (1 mmol) were reacted in dichloromethane with dicyclohexylcarbodiimide (2.2 mmol) and 4-dimethylaminopyridine as catalyst. The mixtures were stirred at room temperature for about 24 h. The products were recrystallized three times from ethanol/toluene and twice from toluene/heptane. Yields: 30–50%. The analytical data are given for compound C12.

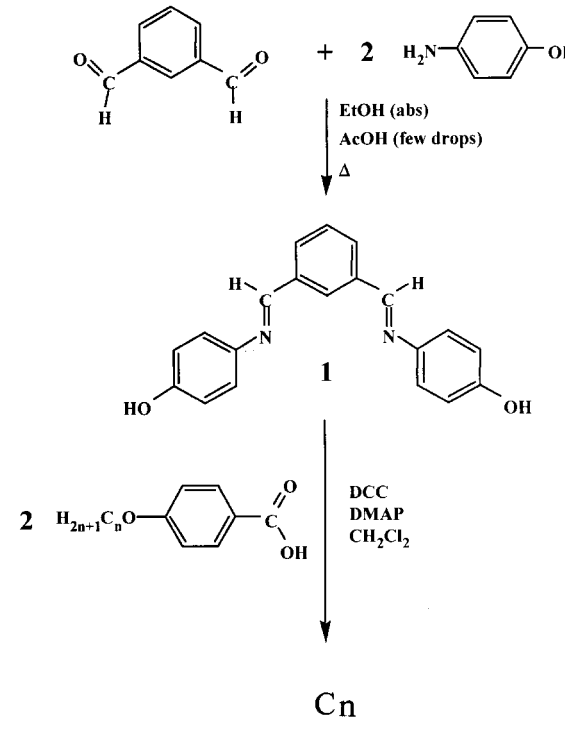

Cn

Figure 1. Synthesis scheme.

^{1}H NMR (200 MHz, $CDCl_3$) δ (ppm): 8.6 (2H, s, CH=N), 8.4 (1H, s, Ar−H), 8.13–8.18 (4H, d, Ar−H), 8.05−8.09 (2H, d,Ar−H), 7.6 (1H, t, Ar−H), 7.2–7.35 (8H, m, Ar−H), 6.95–7.00 (4H, d, Ar−H), 4.05 (4H, t, O−$\underline{CH_2}$), 1.8–1.85 (4H, m, O−CH_2−$\underline{CH_2}$), 1.25–1.5 (36H, m, CH_2), 0.85–0.92 (6H, m, CH3). IR (KBr) ν cm^{-1}: 2920, 2851, 1726, 1606, 1509, 1472, 1289, 1254, 1193, 1170, 1086, 884, 852, 762, 683.

3. Experimental

The thermal behaviour was investigated using a Perkin-Elmer DSC7 differential calorimeter. The optical textures of the mesophases were observed through a polarizing microscope (Leitz Diavert) equipped with a hot stage (FP-82HT) and an automatic controller (Mettler FP-90). Samples were observed on regular slide glass without any surface treatment.

X-ray diffraction experiments on non-oriented samples were performed by using a Guinier film camera. The $CoK_{\alpha 1}$ radiation is selected by a bent quartz monochromator and the scattered radiation collected on film. The experiments on oriented samples were carried out on an 18 kW rotating anode X-ray source (Rigaku-200) with the use of a Ge(1 1 1) crystal as monochromator. The scattered radiation was collected on a two dimensional detector (Imaging Plate system from Mar Research, Hamburg). In both cases, the samples were placed in an oven, providing a temperature control of 0.1 K.

Electro-optical properties were studied using commercial cells (from E.H.C., Japan) with rubbed polyimide layers (but the surface treatment was not effective in making uniformly oriented cells). Switching current was measured by applying a triangular voltage-wave using a function synthesizer (HP 331 20A) and a high power amplifier (Krohn-Hite).

Molecular modeling calculations were performed on a SGI Indy 4400 SC workstation running MacroModel version 5.0 (Columbia University, New York). Conformational minima were found using the modified MM3* (1991 parameters) force field as implemented and completed in the MacroModel program [13]. Calculations were performed with the GB/SA continuum solvation model [14] with chloroform as solvent ($\varepsilon \approx 4$). Built structures were minimized to a final RMS gradient $\leqslant 0.005$ kJ Å^{-1} mol^{-1} via the Truncated Newton Conjugate Gradient (TNCG) method (500 cycles).

A Monte Carlo style conformational search was implemented in MacroModel [15, 16]. The automatic set-up was selected, i.e. single bonds variable, chiral centres set and flexible ring opened. In order to ensure convergence, 3000 steps were made per input structure, in an energy range of 20 kJ mol^{-1} (solution accessible conformations). Each conformer was fully minimized (500 cycles, TNCG method, RMS $\leqslant 0.005$ kJ Å^{-1} mol^{-1}, MM3* force field). The least-used structures were used as starting geometries only if their energies were within the energetic window (20 kJ mol^{-1} of the lowest energy structure yet found). In all cases the extended cut-off option was used (*VdW* = 8 Å, electrostatic = 20 Å and H-bond = 4 Å).

Following the Monte Carlo search, a cluster analysis was performed with XCluster 1.1 [17]. Computational methods used to determine electrostatic potential maps have been recently described [18].

4. Experimental results

4.1. *Basic identification: textures and thermal behaviour*

The transition temperatures and associated enthalpies are listed in table 1. Only one mesophase ('phase 1' or 'phase 2') was observed for each compound of series C.

Figure 2 shows the clearing temperatures T_{cl} as a function of the alkoxy chain length for both the C and I series. The non-regular evolution of T_{cl} suggests two different mesophases depending on the length of the aliphatic terminal chains. According to miscibility studies by the contact method, the mesophases of the C5–C9 homologous on the one hand and of the C10–C14 compounds on the other, are completely miscible with each other indicating one phase for $n \leqslant 9$, and another phase for $n \geqslant 10$. Note that non-symmetric compounds (series I) behave in the same manner and simply exhibit lower transition temperatures.

Table 1. Transition temperatures (°C) and enthalpies (italics, ΔH kJ mol^{-1}) as a function of the number of carbon atoms in the terminal tails (from DSC runs, increasing temperature, rate 5°C min^{-1}).

n	Cr		Phase 1		Phase 2		I
5	•	146.9	•	151.2	—		•
		31.9		*14.2*			
6	•	138.6	•	156.1	—		•
		36.2		*16.3*			
7	•	128.4	•	152.9	—		•
		28.7		*17.2*			
8	•	120.9	•	153.5	—		•
		29.2		*18.2*			
9	•	121.3	•	147.2	—		•
		32.0		*18.8*			
10	•	120.4	—		•	148.9	•
		33.6				*20.1*	
11	•	117	—		•	149.9	•
		37.4				*21.1*	
12	•	115	—		•	151	•
		41.4				*22.3*	
13	•	116.7	—			151.9	•
		72				*23.2*	
14	•	114.8	—		•	150.4	•
		68.5				*23.1*	

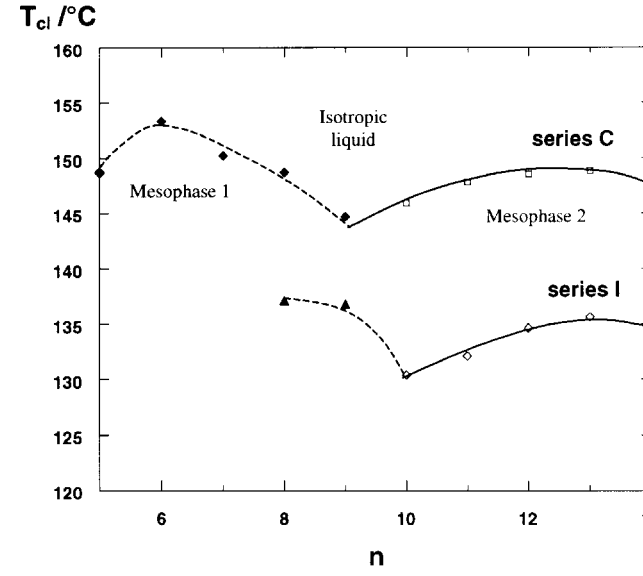

Figure 2. Comparison of the evolution of the clearing temperatures as a function of the alkoxy tail length *n* for both symmetric and non-symmetric series ('C' and 'I', respectively).

The optical textures confirm this distinction: the texture of the mesophase observed for long chain homologues (figure 3(*a*)) is similar to the fringe texture of the B2 mesophase of the PIMB series. The shorter chain homologues (figure 3(*b*)) form a completely different mosaic texture which reminds one of columnar textures [11].

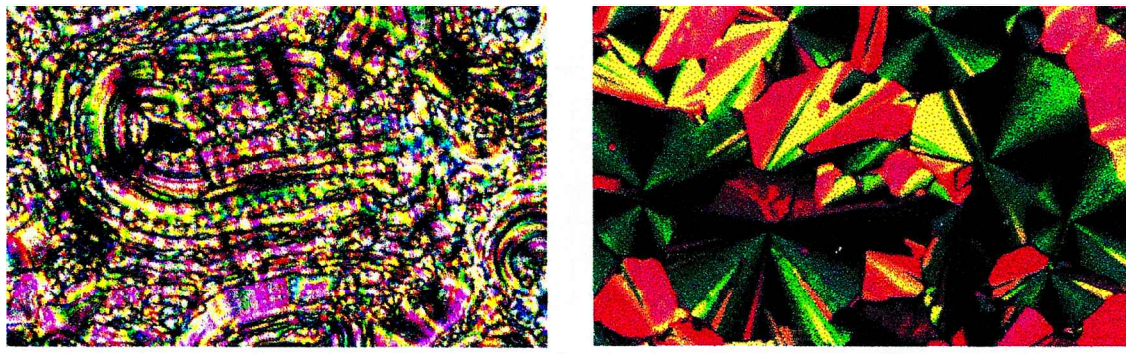

(a) (b)

Figure 3. Textures observed for (*a*) C12 and (*b*) C9 in their mesomorphic state.

For both regimes, the ΔH_{cl} enthalpy changes observed for the clarification transition are larger than the values observed for classical smectic–isotropic transitions of rod-like mesogens or for a rectangular columnar phase to isotropic transition of disc like mesogens ($\approx 4\,kJ\,mol^{-1}$). They are comparable to the values measured in the reference PIMB series [19]. The ΔH_{cl} and ΔS_{cl} values increase regularly on lengthening the terminal chain and no marked discontinuity is observed at the transition between the two regimes (figure 4).

4.2. *X-ray investigations*

The X-ray patterns of C10–C14 show equally-spaced Bragg reflections giving evidence of a layer structure. In addition, a broad diffuse scattering in the wide angle region indicates a 'fluid' smectic with no long range positional order within the layers. Oriented monodomains are obtained by slowly cooling a free droplet from the isotropic state, as shown in figure 5 (*a*); the Bragg reflections and their higher orders are located on the meridian of the pattern. The arrows indicate the direction of the diffuse maxima at wide angles (not visible in the figure due to the large difference in intensity between small and wide angles regions). These diffuse scatterings are situated out of the equator. The angular profile at wide angles, figure 5 (*b*), shows an angle of 94° between the maxima, corresponding to a tilt angle of 42.5° for the C10 compound. According to the experimental accuracy, the tilt angle seems to be quasi-constant in the series (41.5° for C12). Such patterns are consistent with a fluid smectic phase with tilted molecules. In addition, the evolution of the layer spacing d within the C series (figure 6) may be fitted by $d = (1.32n + 22.9)$ Å, where n is the carbon number in each terminal chain. The increment of d is half that expected per methylene group, suggesting that the chains are tilted with reference to the smectic layers.

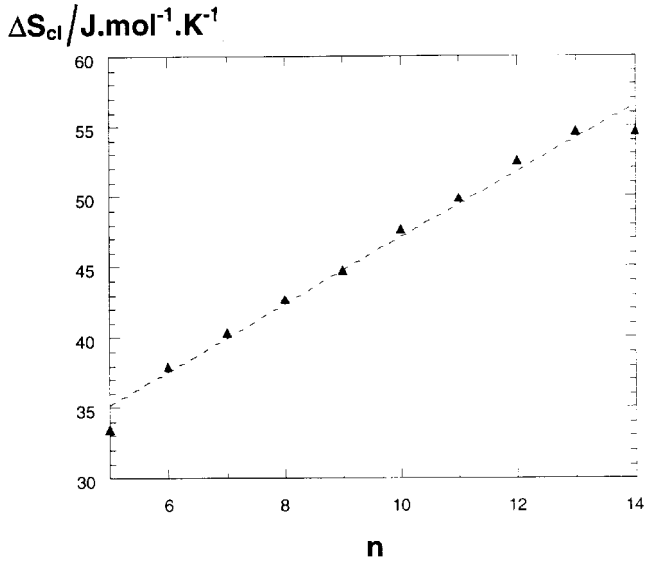

Figure 4. Evolution of the clearing transition entropy ΔS_{Cl} versus the number of carbon atoms n in the terminal chains of series C.

The X-ray patterns of the C5–C9 homologues also exhibit a diffuse scattering at wide angles, showing the absence of in-plane order within the layers. But the small angle region is characterized by two reflections which cannot be assigned to the first and second layer reflections. The ratio of the two parameters increases regularly from 1.22 for $n = 5$ to 1.38 for $n = 9$. Higher orders are probably too weak to be observable. Up to now, we have not obtained a perfect monodomain and thus a structural model of this mesophase cannot be definitely given. Nevertheless, our X-ray patterns share some characteristics with those observed for the B1 phase in the *n*-OPIMB series [19, 20] or for the chloro derivatives [8]. For this reason we undertook miscibility studies between the C*n* compounds and the *n*-OPIMB series.

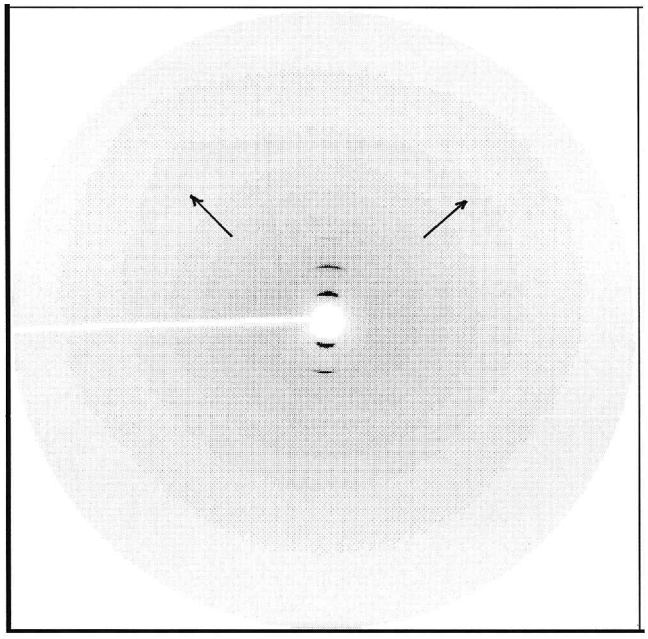

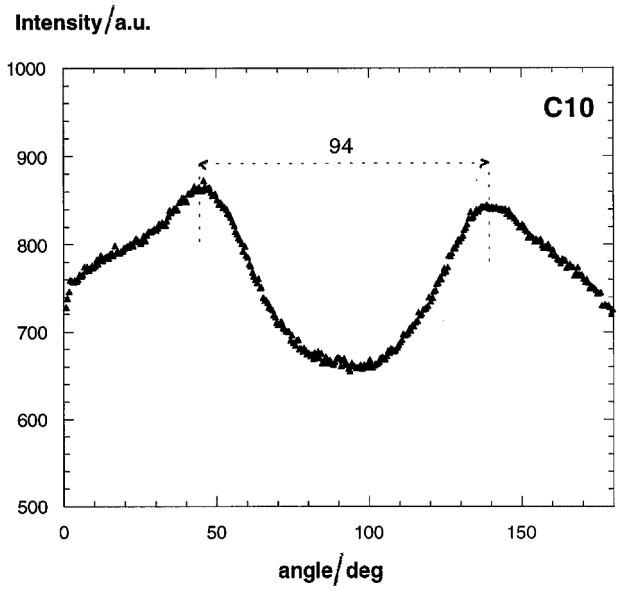

Figure 5. (*a*) X-ray pattern of a monodomain of the C10 compound (146°C); (*b*) corresponding angular intensity profile at wide angles.

4.3. *Miscibility studies*

Figure 7 presents the phase diagram for binary mixtures of the hexyloxy homologue of series C and 6-OPIMB as a reference compound.

The homologue 6-OPIMB exhibits B1, B3 and B4 phases according to the nomenclature proposed at the International Workshop on 'Banana-shaped liquid crystals' (Berlin 1997). B3 is probably a solid phase and B4 a highly reflective blue-coloured phase. The B1 phase is a two dimensional fluid smectic phase with a rectangular lattice [20].

Obviously the mesophase of our C6 compound is miscible with the B1 phase of 6-OPIMB over the whole range of concentrations. The monotonous evolution of the structural parameters associated with the two Bragg reflections which are observed as a function of composition (figure 8) confirms the miscibility. One of these

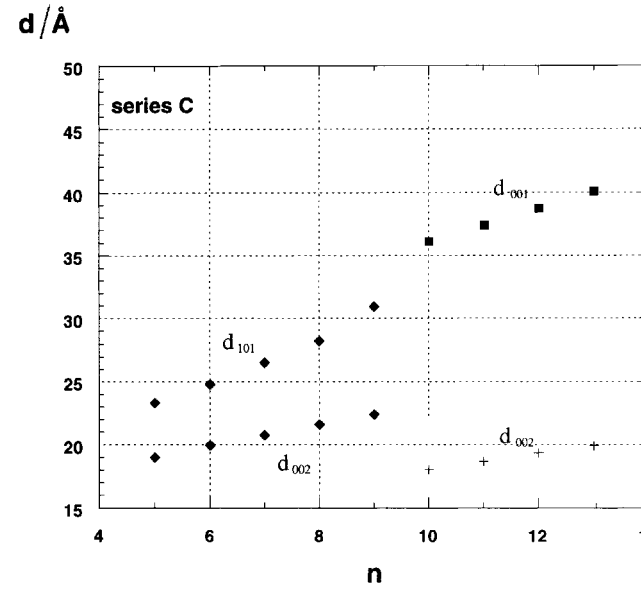

Figure 6. Evolution of the structural parameters *d* as a function of the number of carbon atoms *n* in each of the terminal chains. See text for the indexations of the reflections.

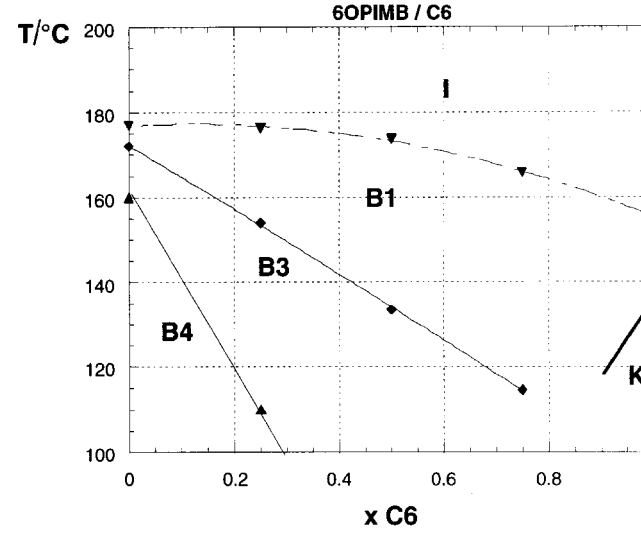

Figure 7. Isobaric temperature–concentration phase diagram for mixtures between 6-OPIMB (left) and the hexyloxy homologue of series C (right).

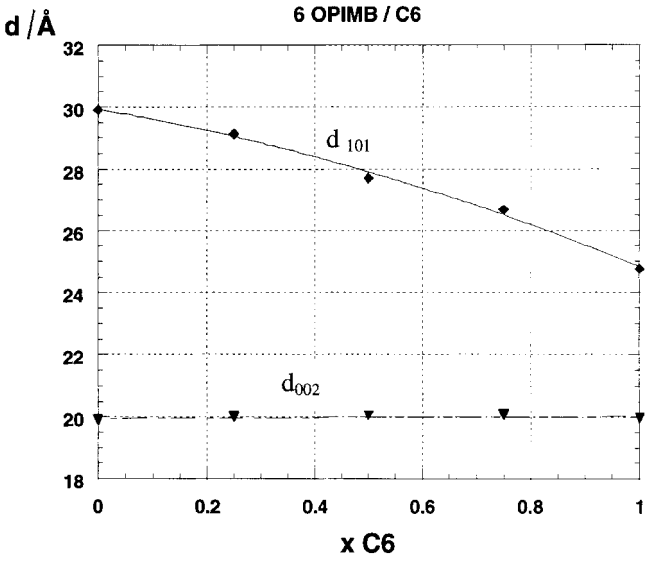

Figure 8. Evolution of the structural parameters in binary mixtures of 6-OPIMB/C6 as a function of composition; 6-OPIMB (left), C6 (right).

corresponding distances stays locked around 20 Å, while the other regularly decreases from 6-OPIMB (30 Å) to C6 (25 Å). Thus, according to the indexing used for the B1 phase of 6-OPIMB (established from samples in which three reflections, indexed as 1 0 1, 0 0 2 and 1 0 3 in reciprocal space, are observed in the low angle region [20]), these two reflections correspond to the 1 0 1 and 0 0 2 indices of an 'antiphase type' rectangular lattice.

The lattice parameter '*c*' corresponding to the layer thickness is constant within the 6-OPIMB/C6 binary diagram (40 Å). Assuming that this thickness is likely to be associated with some characteristic molecular length, the constant value for this parameter over the entire diagram seems consistent with this view since both compounds are expected to be globally isometric. The other two-dimensional lattice parameter '*a*' attributed to the 'in plane' periodicity of the antiphase decreases from 6-OPIMB (44 Å) to C6 (32 Å). This characteristic length is thus dependent on the modification of the molecular arrangement of the linking groups. Finally, one should notice the low value of '*a*' corresponding to a lattice involving less than ten molecules and the absence of higher orders, which suggests a structure that is not well defined. Although the data collected from powder samples prevents a definitive structural characterization, miscibility studies among homologues indicate that the mesophase for all compounds from C5 to C9 appertains to the B1 type. Therefore, we assign the values reported in table 2 to the two dimensional lattice parameters '*c*' and '*a*'.

As illustrated with the electrostatic potential maps of figure 9, the permutation of the linking groups leads to

Table 2. Lattice parameters for a modulated phase with a rectangular lattice, assuming the indexing (0 0 2, 1 0 1): *c* corresponds to the layer thickness and *a* to the in-plane parameter.

n	*c*/Å	*a*/Å
5	38	29.5
6	39.9	32.1
7	41.5	34.5
8	43.2	37.2
9	44.8	38.2

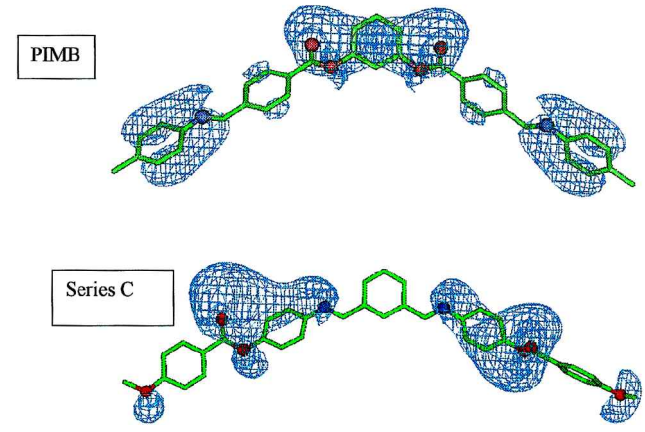

Figure 9. Configuration of PIMB and C compounds resulting from MD and electrostatic potential calculations. Blue contours at $-40\ \mathrm{kJ\ mol^{-1}}$. Molecules are drawn in stick representation with hydrogens omitted for clarity; O and N are represented as balls.

a reversed sequence of charge density from the PIMB to the C series. Despite this change, the behaviour of the binary solutions appears almost ideal: the clearing point equilibrium line (figure 7) shows a very slight curvature and the structural parameters follow a continuous evolution over the entire composition range.

In the same manner, we now compare the smectic phase of the C10–C14 compounds and the B2 phase of the long homologues of the *n*-OPIMB series. The phase diagram of the binary system composed of 12-OPIMB and C12 compounds is shown in figure 10. Complete miscibility of the mesophase of the C12 compound and the B2 phase of 12-OPIMB is clearly evident. Figure 11 shows that the layering spacing regularly (but not linearly) decreases from 12-OPIMB to C12. This feature and the almost perfectly linear evolution of the clarification temperature indicate a kind of ideal behaviour for these smectic solutions.

Note that the B2 phase of the PIMB compounds [6] and chloro substituted derivatives [8] shows a tilt angle of about 35°, and the larger tilt angle observed for the C series can explain the difference in layer spacing between the isometric 12-OPIMB and the C12 compounds.

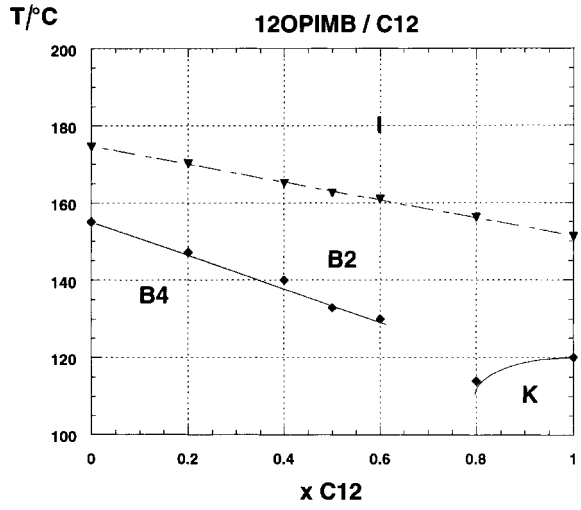

Figure 10. Isobaric temperature–concentration phase diagram from mixtures between 12-OPIMB (left) and the dodecyloxy homologue of series C (right).

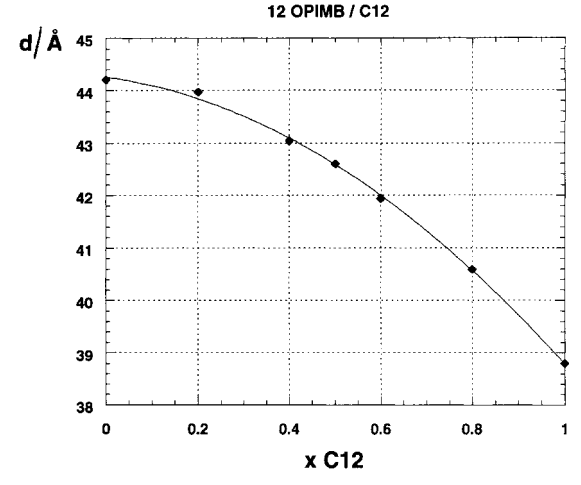

Figure 11. Evolution of the layer spacing as a function of composition in the 12-OPIMB/C12 binary diagram; 12-OPIMB (left), C12 (right).

To summarize, two fluid mesophases are encountered in series C depending on the length of the terminal tail: an antiphase B1 for short homologues (C5–C9) and a smectic phase B2 for long homologues (C10–C14). The striking feature is the fact that no single, pure compound shares the two mesophases. Such a difference also exists for the electro-optic behaviour of the B1 and B2 mesophases.

4.4. *Electro-optic measurements*

The mesophase B1 does not respond to an applied electric field. On the contrary, the B2 smectic phase can be electro-optically switched in accordance with the results obtained for the B2 phase of the PIMB series. We detail below the electro-optic properties of the long homologues C12.

Sample cells were filled by capillary action using the isotropic phase. The 6 μm thick cells from EHC (Japan) were provided with a SiO_2 insulating layer in order to avoid electrical shorts. With the C12 compound and other polar materials, a surface effect occurs as evidenced by extra humps in the switching current curves. This effect still exists in the isotropic phase and may be due to the release of trapped ions or to surface polarization reversal. In order to avoid a rapid decay of the sample purity, all experiments were done under a dry nitrogen atmosphere.

The switching behaviour of the B2 phase was observed in the polarizing microscope simultaneously with the cell current on the oscilloscope screen. Some general trends are seen, complicated by the fact that a uniform alignment was never obtained with this compound. First, the B2 phase grows from the isotropic liquid, the mesophase forming in a rather planar and radial fashion, with new layers that seem to aggregate outside the initially formed islands. In the final structure, one observes a few Maltese crosses surrounded by a fine texture where the layers seem to form concentric structures around the initial centres (figure 12). The entire area outside the crosses can be described as a 'grainy fan-shaped structure' [8], although the grainy character seems to be due to stripes parallel to the layers [5].

When applying a triangular voltage of no more than $\pm 5\,V\,\mu m^{-1}$ at very low frequency, one clearly sees a rotation of the crosses with three different positions for $+V$, 0 and $-V$ voltages; in the meantime no really clear differences in the grainy structure are seen, although the background luminosity changes from place to place. On the oscilloscope screen, one sees a unique peak per half period (figure 13) which, together with the rotation of the Maltese crosses, indicates that the sample is at least partially in a planar unwound chiral smectic C* phase reacting linearly with the field. The outside grainy structure seems to be made of helix-like domains in regions of low curvature of the layers. Inside the cross, highly curved layers appear to induce a completely unwound structure.

With increasing voltage, above a threshold of about $\pm 7\,V\,\mu m^{-1}$, the grainy structure transforms to a striped structure with good contrast and well defined colours, figure 14(*a*). The stripes, apparently periodic in the μm range, are parallel to the layers formed in the nucleation sequence. They resemble so-called 'twins' in solid state physics [21]. For the C12 compound, contrarily to [5, 8], the stripes never disappear even with a voltage up to $\pm 17\,V\,\mu m^{-1}$, probably meaning there is a second threshold above this value which is not reached with our set-up. On shutting down the voltage, the initial

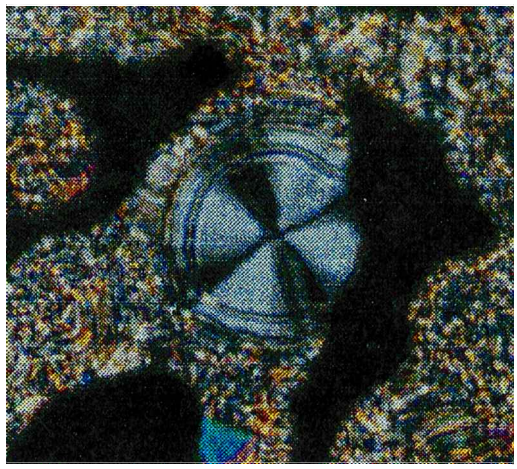

Figure 12. Maltese cross in the B2 phase of the C12 compound ($T = 149°C$) under an applied field ($\pm$ 2.5 V μm^{-1}, 30 mHz).

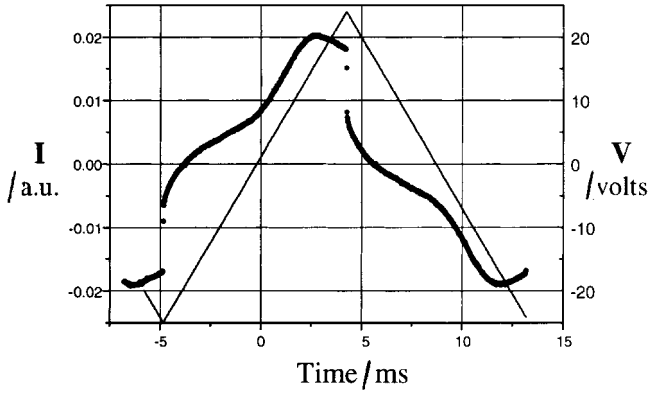

Figure 13. Switching current (I) obtained by applying a triangular voltage V ($\pm$ 4 V μm^{-1}, 55 Hz) at 130°C to the B2 phase of C12, freshly formed from the isotropic liquid.

grainy texture is lost and replaced by a dark grey, nearly uniform texture with some paramorphosis of the striped structure, figure 14 (*b*). This kind of behaviour is reminiscent of a helicoidal smectic C* phase under an applied voltage that partially unwinds the helix. This may confirm the already reported helicoidal character of the B2 phase [22].

In the course of switching with the applied triangular voltage one sees two peaks per half-period (figure 15); one appears simultaneously with the stripes, and the other occurs with the grey texture. It is clear that each peak on the current curve is the signature of a reversible transition between the grey and the striped structures.

This is compatible with a kind of helical structure unwinding partially under increasing voltage and then rewinding under decreasing voltage. The apparent 'saturated polarization' $\mathbf{P}_s$ derived from the area of the peaks (figure 16) is about 350 nC cm^{-2} and is nearly temperature independent, except close to the isotropic phase. Let us note however that this value is underestimated as the striped structure is not fully 'unwound' as with some other banana-shaped mesogens in the B2 phase [5, 8].

To explain our observations, several possibilities exist that can be neither totally confirmed nor ruled out due to the poor quality of the alignment in the cells that restricts the accuracy of the observations. There are clearly two levels of understanding needed. From a microscopic point of view, the arrangement of neighbouring layers, according to Link *et al.*, may be of the ferroelectric/antiferroelectric kind and of the synclinic/anticlinic kind; there are four combinations allowed. From the macroscopic point of view, the striped structure may be explained by a distorted smectic C* helix or by the planar-stripes-model [5].

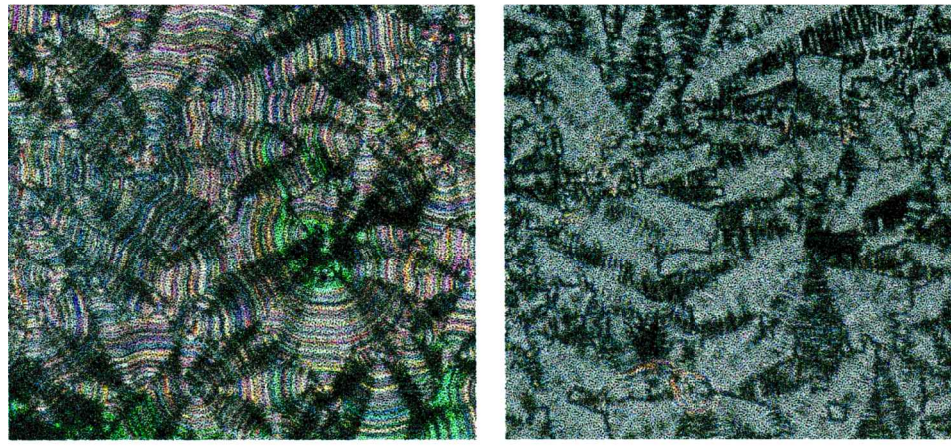

(a) (b)

Figure 14. B2 phase of C12 compound ($T = 140°C$): (*a*) above the threshold ($\pm$ 7 V μm^{-1}), coloured stripes ($\pm$ 17 V μm^{-1}, 30 mHz); (*b*) grey texture, 0 V, same domain as (*a*).

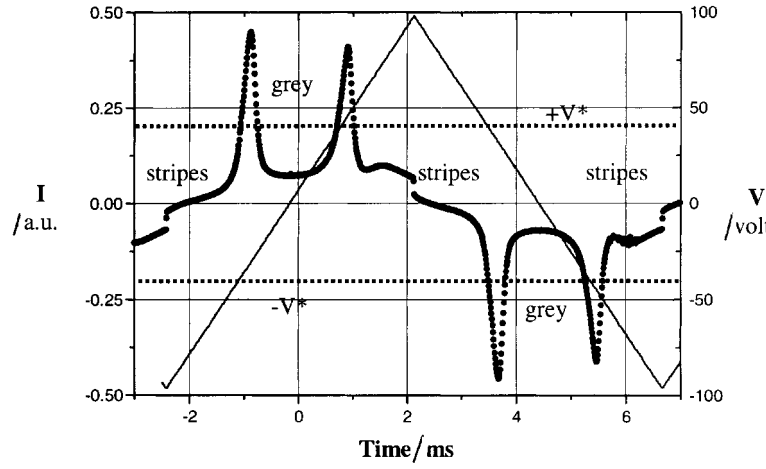

Figure 15. Switching current obtained by applying a triangular voltage ($\pm$ 17 V μm^{-1}, 110 Hz) at 130°C for C12. Note that for a given sign of the voltage slope, the first peak corresponds to a transition from striped to grey structure and the second peak to the reverse transition.

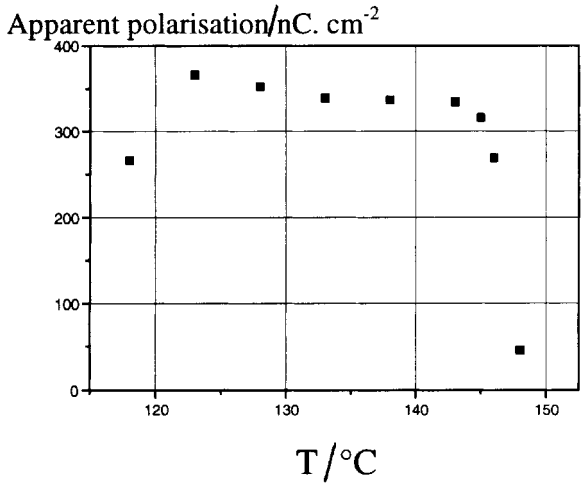

Figure 16. Pseudo-saturated polarisation vs T in the phase B2 of C12.

We cannot discuss seriously the microscopic structure in the absence of uniform alignment. Antiferroelectricity is usually associated with a double peaked switching current curve with triangular voltages. One may show however that there is no absolute obligation for such an association. On the one hand, not all antiferroelectric smectics (A_2, C_A, ...) can switch to a ferroelectric state, and on the other hand, helix unwinding/rewinding or a phenomenon such as a first order smectic A to smectic C* phase transition driven by the field may lead to a multipeaked current curve [23].

From the macroscopic point of view, we are using a would-be SSFLC cell, and a helix partially unwound by the surfaces may be equivalent to the stripe model as soon as planar alignment is favoured. However, the details of the planar-stripes-model do not describe what we observe both with (contrasted stripes) and without (grey texture) applied field. Another analogy should be mentioned with ferrielectric smectics in cells a few μm thick. In a temperature range close to the SmCFi phase, there occurs a demixing of SmC* and SmC^*_A in the form of alternate stripes parallel to the layers [24, 25]. This structure looks like the striped texture we discuss here with alternate colours and polarization reversal under a field; only its aspect without field is different.

The understanding of the grey texture in the field-off regime seems to be of fundamental importance. It is probably due to a low apparent birefringence which is in turn a consequence of some averaging of the intrinsic biaxial indices of the banana-shaped molecules in order to have $n_1 \approx n_2 \approx n_3$. This averaging may be explained by the combination of the rather large bend angle of the molecule, this tilt angle of the smectic phase and helicoidal precession around the layer normal.

Summarizing this section, we favour an interpretation of the observed phenomena in the B2 phase in terms of partial unwinding under the field of a structure which is helicoidal at rest.

5. Concluding remarks

In a new series of banana-shaped mesogens, the two mesophases classified as 'B1' and 'B2' have been clearly identified. The occurrence of one phase or the other appears strongly connected to the length of the aliphatic terminal tails, but is not dependent on the sequence of charges on the phenyl rings. The change between the two regimes occurs abruptly, as shown in the C9–C10 phase diagram through a quasi-vertical biphasic domain (figure 17) as previously observed in the '*In*' series [11]. In addition, one should note the destabilization of both B1 and B2 phases by mixing two homologues which differ only by one carbon atom in the alkoxy chains. This kind of feature makes it difficult to prove non miscibility between B1 and B2 directly through the microscopic contact method. This is the reason why the study of mixtures at given compositions is essential.

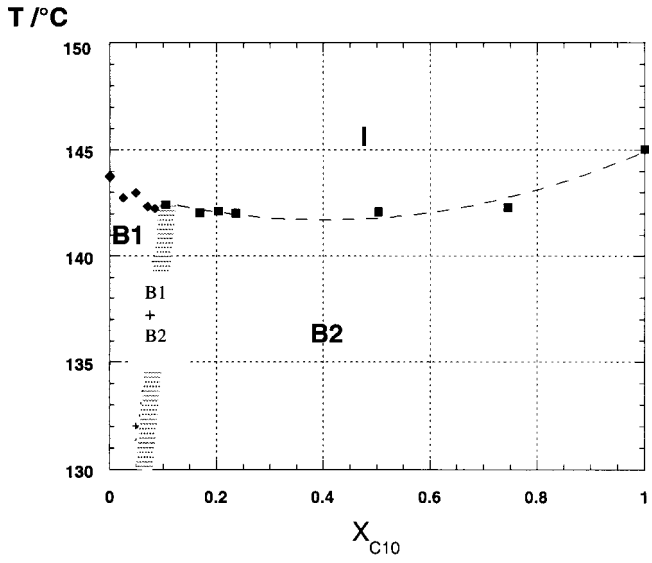

Figure 17. Isobaric temperature–concentration phase diagram from mixtures between the nonyloxy- (left) and the decyloxy- (right) homologue of series C.

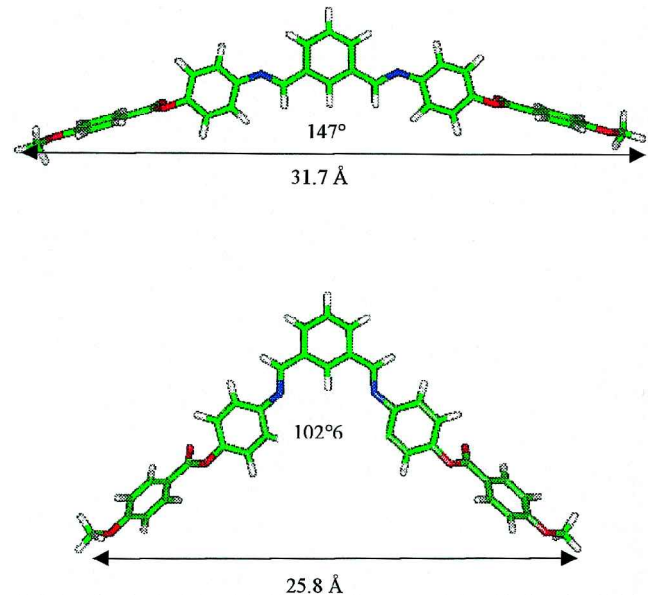

Figure 18. Conformations of a molecule of series C, from molecular mechanics calculations (see experimental part).

Microscopically speaking, one can hypothesize about the molecular origin of these two kinds of mesomorphic arrangement of banana-shaped molecules. One can first note that the molecular organization within a 'banana' mesophase is essentially driven by two kinds of interactions: the electrostatic interactions since the positive and negative charges are strongly localized along the molecule (figure 9), and the van der Waals interactions developed by long aliphatic chains. Several equilibrium states between the different driving forces can be observed depending on the length of the chains and it seems reasonable to envisage distinct possible molecular arrangements according to the length of the terminal chains.

To explain the occurrence of two different mesophases on increasing the length of the terminal chains, one can imagine two possibilities:

(1) A conformation change between short and long homologues. Indeed, molecular mechanics calculations reveal that two energetically favoured conformations exist for an isolated molecule of series C: there correspond either to a bending angle of 147° or to a more V-shaped molecule with an angle of 102°6 (figure 18). The two conformers are separated by an energy gap of only 2.6 kJ mol^{-1}. On this hypothesis, the B1–B2 transition would involve a combined conformational change for a great number of molecules within their liquid crystalline environment and this would cost overall a high energy.

(2) The existence of the same conformation, i.e. the 'same object', with two kinds of molecular arrangement, giving either the layered structure B2 or the two dimensional antiphase B1. Molecular dynamics calculations involving 64 molecules are in progress to obtain a better understanding of the possible local arrangements on varying the molecular parameters of banana-shaped mesogens.

References

[1] Niori, T., Sekine, T., Watanabe, J., Furukawa, T., and Takezoe, H., 1996, *J. mater. Chem.*, **6,** 1231.
[2] Akutagawa, T., Matsunaga, Y., and Yasuhara, K., 1994, *Liq. Cryst.*, **17,** 659.
[3] Niori, T., Sekine, T., Watanabe, J., Furukawa, T., and Takezoe, H., 1997, *Mol. Cryst. liq. Cryst.*, **301,** 337 (Proc. ILCC 96).
[4] Choi, S. W., Kinoshita, Y., Park, B., Takezoe, H., and Niori, T., 1998, *Jpn. J. appl. Phys.*, **37,** 3408.
[5] Link, D. R., Natale, G., Shao, R., Maclennan, J. E., Clark, N. A., Körblova, E., and Walba, D. M., 1997, *Science*, **278,** 1924.
[6] Diele, S., Grande, S., Kruth, H., Lischka, Ch., Pelzl, G., Weissflog, W., and Wirth, I., 1998, *Ferroelectrics*, **212,** 169.
[7] Jàkli, A., Rauch, S., Lötzsch, D., and Heppke, G., 1998, *Phys. Rev. E*, **57,** 6737.
[8] Pelzl, G., Diele, S., Grande, S., Jakli, A., Lischka, Ch., Kresse, H., Schmalfuss, H., Wirth, I., and Weissflog, W., 1999, *Liq. Cryst.*, **26,** 3401.
[9] Vanakaras, A. G., Photinos, D. J., and Samulski, E. T., 1998, *Phys. Rev. E*, **57,** 1.
[10] Nguyen, H. T., Rouillon, J. C., Marcerou, J. P., Bedel, J. P., Barois, P., and Sarmento, S., *Mol. Cryst. liq. Cryst.* (in the press).

[11] Bedel, J. P., Nguyen, H. T., Rouillon, J. C., Marcerou, J. P., Sigaud, G., and Barois, P., *Mol. Cryst. liq. Cryst.* (in the press).
[12] Nguyen, H. T., Rouillon, J. C., Marcerou, J. P., and Barois, P., 1999, Abstracts of the International Conference on Liquid Crystals, Strasbourg (D2-O3).
[13] Mohamadi, F., Richards, N. G. J., Guida, W. C., Liskamp, R., Lipton, M., Caufield, C., Chang, G., Hendrikson, T., and Still, W. C., 1990, *J. comput. Chem.,* **11,** 441.
[14] Still, W. C., Tempczyk, A., Hawley, R. C., and Hendrickson, T., 1990, *J. Am. chem. Soc.*, **112,** 6127.
[15] Chang, G., Guida, W. C., and Still, W. C., 1989, *J. Am. chem. Soc.*, **111,** 4379.
[16] Saunders, M., Houk, K. N., Wu, Y. D., Still, W. C., Lipton, M., Chang, G., and Guida, W. C., 1990, *J. Am. chem. Soc.*, **112,** 1419.
[17] Shenkin, P. S., and McDonald, D. Q., 1994, *J. comput. Chem*, **15,** 899.
[18] Hardouin, F., Achard, M. F., Laguerre, M., Jin, J.-I., and Ko, D.-H., 1999, *Liq. Cryst.*, **26,** 589.
[19] Sekine, T., Niori, T., Sone, M., Watanabe, J., Choi, S. W., Takanishi, Y., and Takezoe, H., 1997, *Jpn. J. appl. Phys.*, **36,** 6455.
[20] Watanabe, J., Niori, T., Sekine, T., and Takezoe, H., 1998, *Jpn. J. appl. Phys.*, **37,** L139.
[21] Kittel, C., 1956, *Introduction to Solid State Physics* (New York: Wiley).
[22] Sekine, T., Niori, T., Watanabe, J., Furukawa, T., Choi, S. W., and Takezoe, H., 1997, *J. mater. Chem.*, **7,** 1307.
[23] Dupont, L., Galvan, J. M., Marcerou, J. P., and Prost, J., 1988, *Ferroelectrics*, **84,** 317.
[24] Gorecka, R., Chandani, A. D. L., Ouchi, Y., Takezoe, H., and Fukuda, A., 1990, *Jpn. J. appl. Phys.*, **29,** 131.
[25] Cluzeau, P., 1995, PhD thesis, University of Bordeaux I, France.